Synthesis and Morphology Control of Gold/Iron Oxide Magnetic Nanocomposites via a Simple Aqueous Method

L. Li[1], K. Y. Mak[1], C. W. Leung[2], C. H. Leung[1], A. Ruotolo[3], K.Y. Chan[4], W. K. Chan[4], and P. W. T. Pong[1]

[1]Department of Electrical and Electronic Engineering, The University of Hong Kong, Hong Kong
[2]Department of Applied Physics, Hong Kong Polytechnic University, Hong Kong
[3]Department of Physics and Materials Science, City University of Hong Kong, Hong Kong
[4]Department of Chemistry, The University of Hong Kong, Hong Kong

Gold/iron oxide nanocomposites offer the promise of combining the unique traits of both gold and iron oxide nanomaterials to enable new applications. In this work, a simple and safe method has been established whereby the morphology of gold material in gold/iron oxide nanocomposites can be controlled to be nanowire or nanosphere by adjusting the initial molar ratio of citrate-coated iron oxide nanoparticles to auric acid. Gold/iron oxide nanowires and nanospheres were synthesized through this method. Their structural, optical, and magnetic properties were characterized by transmission electron microscopy (TEM), energy-dispersive X-ray spectroscopy (EDS), dynamic light scattering (DLS), ultraviolet-visible spectroscopy (UV-Vis), and vibrating sample magnetometry (VSM). These materials substantially maintained the optical properties of gold nanomaterials and magnetic features of iron oxide magnetic nanoparticles.

***Index Terms*—Gold, iron oxide, morphology control, nanosphere, nanowire.**

I. Introduction

NANOCOMPOSITES, being composed of two or more different functional components, have attracted increasing interest from material scientists due to their combined physicochemical properties inherited from constituent components. Two important nanomaterials are gold and iron oxide, whose complementary properties offer the promise of enabling new applications if combined together. Gold nanomaterials exhibiting very interesting physicochemical and optoelectronic properties have been widely used in catalysis, hyperthermia, biosensing, and optics applications [1]–[3]. Their properties, such as plasmon band positions, enhancements in surface enhanced Raman scattering, catalysis abilities, and so forth, can be modulated by tuning their geometries [4]. One of the more interesting gold-based products is to combine gold and iron oxide together to achieve magnetic gold/iron oxide nanocomposites, which has advantages of magnetic separation from precursor materials or as hyperthermia agents in both alternating magnetic field and near infra-red field [5], [6]. Therefore, many researchers have focused on the fabrication of the gold/iron oxide nanocomposites in order to develop multifunctional materials that possess the advantageous properties from both gold and iron oxide [7].

In the past decade, magnetic gold/iron oxide nanocomposites in various morphologies have been synthesized [5], [8]–[15]. Sun's group prepared gold/iron oxide dumbbell nanocomposites and nanoflowers composed of gold nanospheres [8], [9]. Seino *et al.* achieved aggregate composites consisting of iron oxide nanoparticle and gold nanospheres [10], [11]. Wang *et al.* used a solvothermal method to synthesize iron oxide/gold core/satellite nanocomposites composed of gold nanospheres [12]. Levin *et al.* and Pal *et al.* fabricated Fe_xO_y@Au core/shell nanoparticles constituted by gold nanoshells [13], [14]. Gole *et al.* reported a process to generate an iron oxide coating around gold nanorods [5]. These gold nanorod and iron oxide nanoparticle composites were synthesized for use as multifunctional magnetic-optical probes by Wang and Irudayaraj [15]. However, only one type of morphology of the gold components (nanosphere, nanoshell, or nanorod) can be achieved in the final products through each of these reported methods. None of the reports so far have demonstrated a synthesis method which enables controllable variation of gold morphology in the magnetic gold/iron oxide nanocomposites, for example, magnetic nanocomposites with gold nanowires or magnetic nanocomposites with gold nanospheres. The reported methods do not allow the selection of gold morphology by adjusting the process parameters.

Herein, we demonstrate a simple aqueous approach to synthesize gold/iron oxide nanocomposites with tunable morphologies of gold material. The gold/iron oxide nanocomposites are fabricated through the addition of sodium citrate solution containing citrate-coated iron oxide nanoparticles into boiled auric acid, by taking full advantage of the multiple-roles played by citrate in the synthesis process: surface modification of iron oxide nanoparticles, reducing reagent of Au^{3+}, and protection groups. In this paper, the morphology of the gold component in the final gold/iron oxide nanocomposites can be controlled to be nanowire or nanosphere by adjusting the initial molar ratio of citrate-coated iron oxide nanoparticles added to auric acid. The morphology of the resulting nanocomposites is explored for multiple molar ratios of initial chemical reagents, and then the optical and magnetic properties were characterized to demonstrate the robustness of this synthesis technique.

II. Experiment

A. Materials

Ferric chloride hexahydrate ($FeCl_3 \cdot 6H_2O$), ferrous sulfate heptahydrate ($FeSO_4 \cdot 7H_2O$), sodium hydroxide (NaOH), citric

Manuscript received April 28, 2013; revised July 02, 2013; accepted July 19, 2013. Date of current version December 23, 2013. Corresponding author: P. W. T. Pong (e-mail: ppong@eee.hku.hk).

Color versions of one or more of the figures in this paper are available online at http://ieeexplore.ieee.org.

Digital Object Identifier 10.1109/TMAG.2013.2274457

0018-9464 © 2013 IEEE

acid ($C_6H_8O_7$), auric acid ($HAuCl_4$), sodium citrate tribasic dihydrate ($Na_3C_6H_5O_7{\cdot}2H_2O$), and hydrochloric acid (HCl) were purchased from Sigma-Aldrich (USA). All chemicals were used as received. All glassware was cleaned in a bath of freshly prepared aqua regia solution (HCl/HNO_3, 3:1), then rinsed thoroughly with MilliQ water prior to use.

B. Synthesis of Citrate-Coated Iron Oxide Nanoparticles

The iron oxide nanoparticles (IONPs) were synthesized based on coprecipitation of aqueous solutions containing $FeSO_4 \cdot 7H_2O$ and $FeCl_3 \cdot 6H_2O$ (molar ratio of $Fe^{2+} : Fe^{3+} = 1 : 2$) by sodium hydroxide [16]. Then the IONPs were heated to 363 K with the presence of citric acid and trisodium citrate under the pH value of 4 [17]. Under continuous stirring for 1 hour, citrate-coated iron oxide nanoparticles (CIONPs) were obtained. MilliQ water was added to adjust the concentration of the final solution to 50 mM CIONPs (approximately 50 mM trisodium citrate and 50 mM IONPs).

C. Synthesis of Gold/Iron Oxide Magnetic Nanowires and Nanospheres

A typical reaction is as follows. A 20-mL sample of $HAuCl_4$ (0.25 mM) was prepared and brought to boil. Next, a 50 mM CIONP solution was then rapidly added to achieve the desired $CIONPs/HAuCl_4$ molar ratio, and then the mixture was heated further for 10 min. The heat source was then removed and the solution was allowed to cool to room temperature. The gold/iron oxide nanocomposites were collected by magnetic attraction and washed with MilliQ water. For this study, the initial $CIONPs/HAuCl_4$ molar ratios (denoted as R) were 1, 2, 5, 7, and 10. Pure gold nanoparticles (AuNPs) for use as experimental control were synthesized through the reduction of $HAuCl_4$ using 1 mL of 50 mM sodium citrate solution.

D. Characterization

Transmission electron microscopy (TEM, FEI Tecnai G2 20 S-TWIN) was used to characterize both the size and morphology of the synthesized nanocomposites. The chemical components of the nanocomposites were analyzed through energy-dispersive X-ray spectroscopy (EDS) microanalysis. For both TEM and EDS analysis, samples were prepared by dispensing dilute drops of the nanocomposite suspension on carbon-coated copper grids and allowed to dry slowly. Dynamic light scattering (DLS) was performed to measure the hydrodynamic sizes of the nanocomposites dispersed in water using a Malvern Zetasizer 3000 (Malvern, U.K.). The ultraviolet-visible (UV-Vis) absorbance spectra of the nanocomposites in water were recorded with a Hewlett-Packard (model 8453) spectrophotometer. The magnetic properties of lyophilized samples were carried out using a vibrating sample magnetometer (Lakeshore, VSM 7400) at $T = 100$ K and $T = 300$ K.

III. Results and Discussion

The morphology and chemical components of the as-synthesized products were first investigated by TEM and EDS. The gold/iron oxide nanocomposites produced from different initial molar ratios of $CIONPs/HAuCl_4$ displayed varied morphologies under TEM observation [Fig. 1(a)–(e)]. When $R = 1$, the gold nuclei [as indicated by red arrows in Fig. 1(a)] appeared around the iron oxide nanoparticles and together they formed gold nuclei/iron oxide nanoparticle aggregates [Fig. 1(a)]. When $R = 2$, the gold nuclei displayed significant growth around the iron oxide nanoparticles [indicated by red arrows in Fig. 1(b)]. This morphology then transformed into twisted gold nanowires mixed with the iron oxide nanoparticles when $R = 5$ [Fig. 1(c)]. When the molar ratio increased to 7, the nanocomposite morphology consisted of a mixture of longer and thicker gold nanowire networks surrounded with iron oxide nanoparticles formed as shown in Fig. 1(d). Gold nanospheres were also observed at this ratio [indicated by red arrows in Fig. 1(d)]. As R reached 10, the morphology of the products finally changed to gold nanospheres surrounded by iron oxide nanoparticles as shown in Fig 1(e). The presence of gold and iron oxide was confirmed by EDS measurements, and a representative EDS result ($CIONPs/HAuCl_4$ ratio at $R = 1$) is shown in Fig. 1(f).

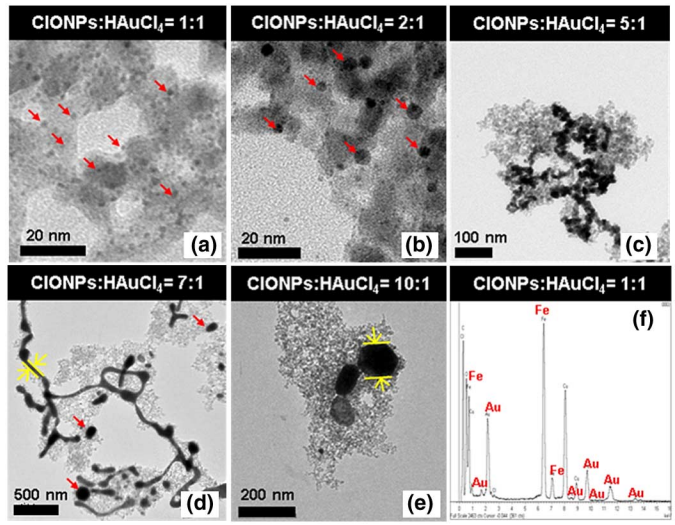

Fig. 1. TEM images (a)–(e) of gold/iron oxide nanocomposites synthesized by different initial molar ratio of citrate-coated iron oxide nanoparticles (CIONPs) to auric acid ($HAuCl_4$) but with fixed reaction time of 10 min. (f) EDS result for the sample when the molar ratio of CIONPs : $HAuCl_4$ is 1:1. Elements of Au and Fe are labeled (color online).

The hydrodynamic sizes (Z-average size) of the nanocomposites in water were examined by DLS. Consistent with the varied shapes observed by TEM, the hydrodynamic sizes of the as-synthesized products show nonlinear relation with the initial molar ratio R of $CIONPs/HAuCl_4$ as shown in Fig. 2(a). The Z-average sizes of gold/iron oxide nanocomposites were 431.4 nm ($R = 1$), 693.4 nm ($R = 2$), and 753.5 nm ($R = 5$) respectively. When R was 7, the DLS measurement was not applicable, due to the formation of large gold nanowires networks which caused the aggregation of nanocomposites into large clusters with hydrodynamic sizes of micrometers. This is supported by the observation from the TEM image in Fig. 1(d). However, when R further increased to 10, the hydrodynamic size of the nanocomposites decreased to 393.3 nm. This could be explained by the morphological change of the final products

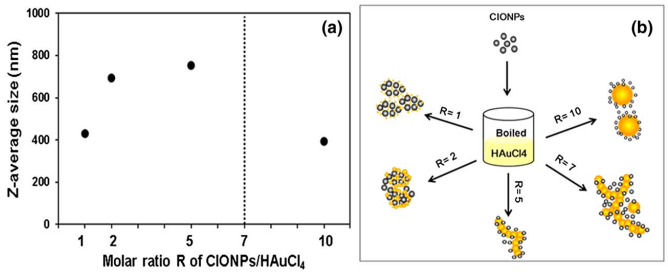

Fig. 2. (a) Hydrodynamic size (Z-average size) and (b) schematic illustration of gold/iron oxide nanocomposites synthesized by varying initial molar ratio R of citrate-coated iron oxide nanoparticles (CIONPs) to auric acid ($HAuCl_4$) but with fixed reaction time of 10 min. Dashed lines are provided as visual guides (color online).

to the gold nanospheres surrounded with iron oxide nanoparticles, and these final products displayed much smaller size than the gold nanowire networks.

The different morphologies of gold/iron oxide nanocomposite with different initial ratio between CIONPs and $HAuCl_4$ are schematically described in Fig. 2(b). The morphological change of the gold nanomaterial (from nuclei to nanowire, then to nanosphere) through citrate reduction of $AuCl_4^-$ has been reported by other research groups [18], [19]. They proposed a growth mechanism about the reduction process of aqueous $AuCl_4^-$ by sodium citrate: nucleation stage, fast random attachment to form nanowire network, growth of nanowires accompanied by fragmentation of network, and cleaving of spherical-like particles. By extracting reaction solution at different time points and rapid cooling with ice to quench the reduction of $AuCl_4^-$, gold nanomaterials with different morphologies were achieved in their experiments due to the noncomplete reduction. In our experiment, the morphological changes of the nanocomposites with different initial molar ratio of CIONPs/$HAuCl_4$ could also be explained by the noncomplete reduction of $AuCl_4^-$ due of insufficient CIONPs. Nanocomposites synthesized at lower initial molar ratios were provided with less CIONPs and thus the reduction process could not be complete within 10 min. At higher molar ratios, the nanocomposites were provided with more CIONPs during reduction, resulting in the different morphologies of the nanocomposites observed.

To adjust the constituent ratio of gold and iron in the nanocomposites, the excess iron oxide nanoparticles in the products could be removed by HCl wash. Here, the nanocomposites achieved with $R = 7$ [Fig. 1(d)] and $R = 10$ [Fig. 1(e)] were washed by 1.2 N HCl twice, collected by magnetic attraction, and then redispersed in MilliQ water. The final gold/iron oxide nanowires (AuIO-NW, $R = 7$) and nanospheres (AuIO-NS, $R = 10$) were obtained as shown in Fig. 3(a) and (b), respectively. EDS results of AuIO-NW and AuIO-NS confirm the presence of gold and iron oxide [Fig. 3(a1) and (b1)]. The CIONPs [Fig. 3(c)] and AuNPs [Fig. 3(d)] synthesized as described in the experiment section served as control. The selected area diffraction pattern [the inset in Fig. 3(c)] demonstrates the CIONPs show a characteristic diffraction pattern of the magnetite nanoparticles. The size distribution for CIONPs [Fig. 3(c1)] and AuNPs [Fig. 3(d1)]

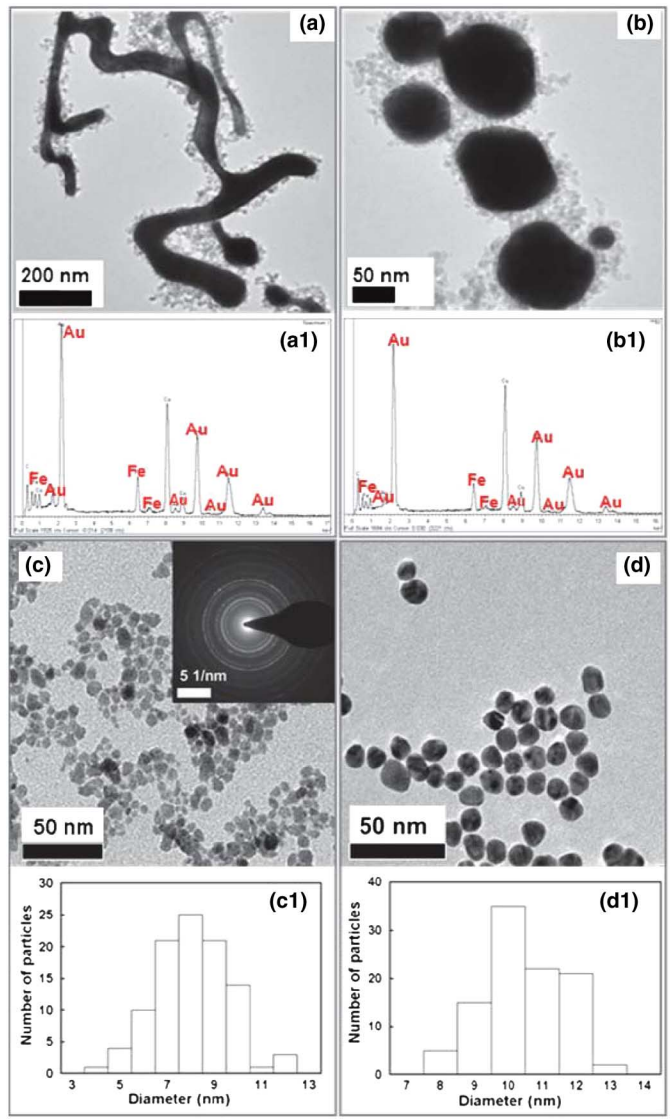

Fig. 3. TEM images of (a) gold/iron oxide nanowires (AuIO-NW, $R = 7$, after HCl wash) and (b) gold/iron oxide nanospheres (AuIO-NS, $R = 10$, after HCl wash). EDS result of (a1) AuIO-NW and (b1) AuIO-NS. Elements of Au and Fe are labeled. TEM images of (c) citrate-coated iron oxide nanoparticles (CIONPs), and (d) gold nanoparticles (AuNPs). Inset in (c) shows a characteristic diffraction pattern of the magnetite nanoparticles. Histogram of the particles sizes of (c1) CIONPs and (d1) AuNPs (color online).

was determined by manually measuring the diameters of the nanoparticles from their TEM images. The iron oxide cores of CIONPs show a size of 7.6 ± 1.6 nm, while the AuNPs show a size of 10.0 ± 1.3 nm.

Next, to demonstrate the possibility of these gold/iron oxide nanocomposites working as a bifunctional material, we measured both their magnetic and optical properties. The magnetic properties of the AuIO-NW, AuIO-NS, and CIONPs were characterized by VSM. The magnified views of M-H loops normalized by the saturation magnetization at 100 K and 300 K are shown in Fig. 4(a) and (b), respectively. They all exhibit superparamagnetic behavior at $T = 300$ K. The appearance of coercivities in Fig. 4(b) indicates that all three samples are in the blocked state at $T = 100$ K. The measured coercivities are $Hc = 110$ Oe for the AuIO-NW and $Hc = 40$ Oe

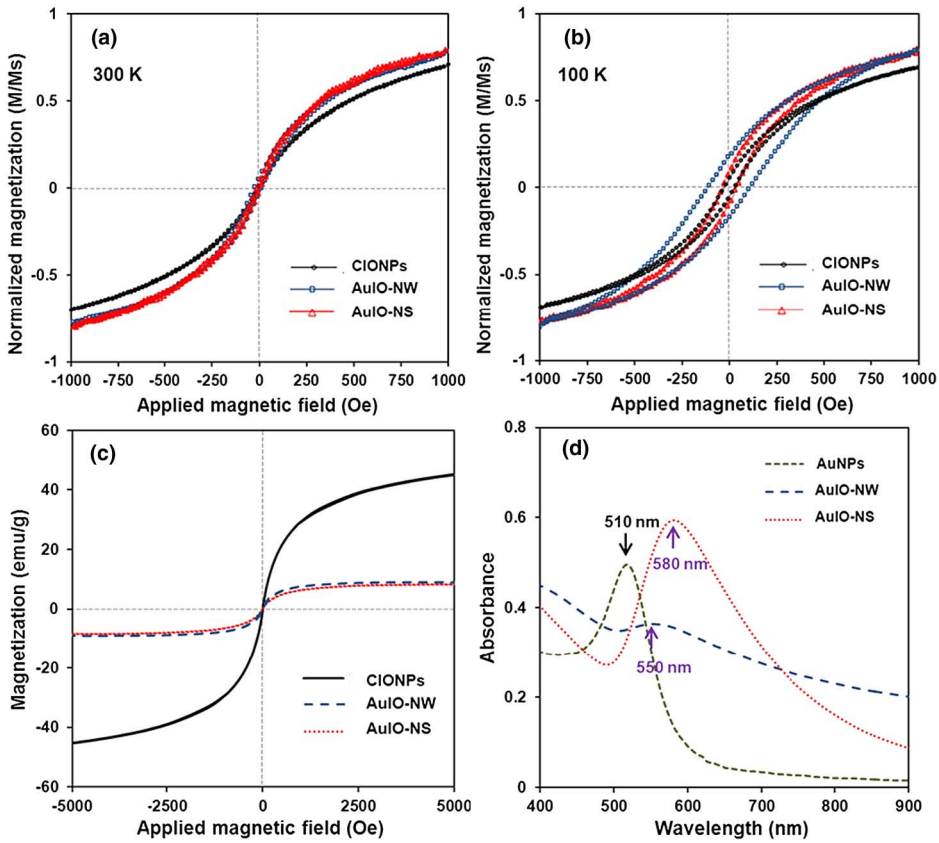

Fig. 4. VSM characterization of the synthesized citrate-coated iron oxide nanoparticles (CIONPs), gold/iron oxide nanowires (AuIO-NW, $\mathrm{R} = 7$, after HCl wash), and gold/iron oxide nanospheres (AuIO-NS, $\mathrm{R} = 10$, after HCl wash). Magnified views of the M-H loops normalized by the saturation magnetization at 300 K and 100 K are shown in (a) and (b) respectively. Full view of the M-H loop at 300 K is shown in (c). (d) UV-Vis absorbance spectrum of synthesized gold nanoparticles (AuNPs), AuIO-NW, and AuIO-NS (color online).

for the AuIO-NS, which are both larger than $\mathrm{Hc} = 25$ Oe of the parent CIONPs. A possible mechanism is the direct interaction between gold and iron oxide nanoparticles proposed by Matthew *et al.* who also observed the increased coercivity of gold-magnetite nanocomposite than untreated magnetite at low temperature [20]. As shown in Fig. 4(c), the saturation magnetization ($\mathrm{M_S}$) values of AuIO-NW (8.99 emu/g) and AuIO-NS (8.32 emu/g) at $\mathrm{T} = 300$ K (near room temperature) are all less than the $\mathrm{M_S}$ of the CIONPs (45.53 emu/g) due to the presence of the nonmagnetic gold in the sample, but are comparable with the $\mathrm{M_S}$ value (~ 5 emu/g) of the gold/magnetite nanocomposites formed via other methods [20]. Although the AuIO-NW and AuIO-NS displayed different morphologies, they exhibited very similar $\mathrm{M_S}$ values here which indicate that the gold contents are with similar ratios within the end products.

The optical features of these AuIO-NW and AuIO-NS were characterized by UV-Vis spectra [Fig. 4(d)]. Their absorbance peaks [indicated by purple arrows in Fig. 4(d)] are shifted to the right from the absorbance peak of pure gold nanoparticles (~ 510 nm) because of the larger gold nanowires and nanospheres formed in the AuIO-NW and the AuIO-NS compared to the pure gold nanoparticles [~ 10 nm in Fig. 3(d)]. The shifts of the absorbance peaks are consistent with the UV-Vis spectra observed by another research group for pure gold nanowire networks and pure gold nanoparticles [19]. The magnetic and optical properties indicate that both AuIO-NW and AuIO-NS can serve as an efficient bi-functional material.

IV. Conclusion

Here, a straightforward method was established for the fabrication of the gold/iron oxide nanocomposites based on the reduction of $\mathrm{HAuCl_4}$ by CIONPs in aqueous situation. We demonstrated that the morphologies of gold/iron oxide nanocomposites could be controlled by adjusting the molar ratio of CIONPs/$\mathrm{HAuCl_4}$. As such, gold/iron oxide nanocomposites with nanowire or nanosphere morphologies can be successfully synthesized. Further, nanocomposites synthesized with this method as both AuIO-NW and AuIO-NS have been shown to substantially maintain the optical properties of gold nanoparticles and the magnetic features of iron oxide nanoparticles. The combined functionalities may have potential use in applications, such as magnetic photothermal therapy reagent and recyclable nanocatalysis.

Acknowledgment

This work was supported in part by the Seed Funding Program for Basic Research and Small Project Funding Program from the University of Hong Kong, ITF Tier 3 funding (ITS/

112/12), by RGC-GRF under Grant (HKU 704911P), and by the University Grants Committee of Hong Kong under Contract AoE/P-04/08. Assistance from F. Chan (EMU, HKU) on TEM examination and assistance from X. Wang (City University of Hong Kong) on VSM measurement are gratefully acknowledged. The authors would like to thank Dr. C. Roberts for proofreading the manuscript.

REFERENCES

[1] M. Chirea, A. Freitas, B. S. Vasile, C. Ghitulica, C. M. Pereira, and F. Silva, "Gold nanowire networks: Synthesis, characterization, and catalytic activity," *Langmuir*, vol. 27, pp. 3906–3913, 2011.

[2] E. Boisselier and D. Astruc, "Gold nanoparticles in nanomedicine: Preparations, imaging, diagnostics, therapies and toxicity," *Chemical Soc. Rev.*, vol. 38, pp. 1759–1782, 2009.

[3] J. M. Nam, C. S. Thaxton, and C. A. Mirkin, "Nanoparticle-based bio-bar codes for the ultrasensitive detection of proteins," *Science*, vol. 301, pp. 1884–1886, 2003.

[4] E. S. Kooij, W. Ahmed, C. Hellenthal, H. J. W. Zandvliet, and B. Poelsema, "From nanorods to nanostars: Tuning the optical properties of gold nanoparticles," *Colloids and Surfaces A: Physicochemical Eng. Aspects*, vol. 413, pp. 231–238, Nov. 5, 2012.

[5] A. Gole, J. W. Stone, W. R. Gemmill, H. C. zur Loye, and C. J. Murphy, "Iron oxide coated gold nanorods: Synthesis, characterization, and magnetic manipulation," *Langmuir*, vol. 24, pp. 6232–6237, 2008.

[6] C. Hoskins, Y. Min, M. Gueorguieva, C. McDougall, A. Volovick, and P. Prentice *et al.*, "Hybrid gold-iron oxide nanoparticles as a multifunctional platform for biomedical application," *J. Nanobiotechnol.*, vol. 10, p. 27, 2012.

[7] K. C. F. Leung, S. Xuan, X. Zhu, D. Wang, C. P. Chak, and S. F. Lee *et al.*, "Gold and iron oxide hybrid nanocomposite materials," *Chemical Soc. Rev.*, vol. 41, pp. 1911–1928, 2012.

[8] H. Yu, M. Chen, P. M. Rice, S. X. Wang, R. L. White, and S. Sun, "Dumbbell-like bifunctional $Au - Fe_3O_4$ nanoparticles," *Nano Lett.*, vol. 5, pp. 379–382, Feb. 01, 2005.

[9] J. Xie, F. Zhang, M. Aronova, L. Zhu, X. Lin, and Q. Quan *et al.*, "Manipulating the power of an additional phase: A flower-like $Au - Fe_3O_4$ optical nanosensor for imaging protease expressions in vivo," *ACS Nano*, vol. 5, pp. 3043–3051, Apr. 26, 2011.

[10] S. Seino, T. Kusunose, T. Sekino, T. Kinoshita, T. Nakagawa, and Y. Kakimi *et al.*, "Synthesis of gold/magnetic iron oxide composite nanoparticles for biomedical applications with good dispersibility," *J. Applied Phys.*, vol. 99, pp. 08H101–08H101-3, 2006.

[11] S. Seino, T. Kinoshita, T. Nakagawa, T. Kojima, R. Taniguci, and S. Okuda *et al.*, "Radiation induced synthesis of gold/iron-oxide composite nanoparticles using high-energy electron beam," *J. Nanoparticle Res.*, vol. 10, pp. 1071–1076, Aug. 01, 2008.

[12] Y. Wang, Y. Shen, A. Xie, S. Li, X. Wang, and Y. Cai, "A simple method to construct bifunctional Fe_3O_4/Au hybrid nanostructures and tune their optical properties in the near-infrared region," *J. Physical Chemistry C*, vol. 114, pp. 4297–4301, 2010.

[13] C. S. Levin, C. Hofmann, T. A. Ali, A. T. Kelly, E. Morosan, and P. Nordlander *et al.*, "Magnetic–plasmonic core–shell nanoparticles," *ACS Nano*, vol. 3, pp. 1379–1388, Jun. 23, 2009.

[14] S. Pal, M. Morales, P. Mukherjee, and H. Srikanth, "Synthesis and magnetic properties of gold coated iron oxide nanoparticles," *J. Applied Phys.*, vol. 105, pp. 07B504-07B504–3, 2009.

[15] C. Wang and J. Irudayaraj, "Multifunctional magnetic–optical nanoparticle probes for simultaneous detection, separation, and thermal ablation of multiple pathogens," *Small*, vol. 6, pp. 283–289, 2009.

[16] R. Massart, "Preparation of aqueous magnetic liquids in alkaline and acidic media," *IEEE Trans. Magn.*, vol. 17, no. 6, pp. 1247–1248, Dec. 1981.

[17] P. Morais, R. Santos, A. Pimenta, R. Azevedo, and E. Lima, "Preparation and characterization of ultra-stable biocompatible magnetic fluids using citrate-coated cobalt ferrite nanoparticles," *Thin Solid Films*, vol. 515, pp. 266–270, 2006.

[18] B. K. Pong, H. I. Elim, J. X. Chong, W. Ji, B. L. Trout, and J. Y. Lee, "New insights on the nanoparticle growth mechanism in the citrate reduction of gold (III) salt: Formation of the Au nanowire intermediate and its nonlinear optical properties," *J. Physical Chemistry C*, vol. 111, pp. 6281–6287, 2007.

[19] X. Ji, X. Song, J. Li, Y. Bai, W. Yang, and X. Peng, "Size control of gold nanocrystals in citrate reduction: The third role of citrate," *J. Amer. Chemical Soc.*, vol. 129, pp. 13939–13948, 2007.

[20] A. Pradhan, R. C. Jones, D. Caruntu, C. J. O'Connor, and M. A. Tarr, "Gold–magnetite nanocomposite materials formed via sonochemical methods," *Ultrasonics Sonochemistry*, vol. 15, pp. 891–897, 2008.